NEUROSCIENCE

A neural substrate of compulsive alcohol use

Esi Domi[1]*†, Li Xu[1,2†], Sanne Toivainen[1], Anton Nordeman[1], Francesco Gobbo[3], Marco Venniro[4], Yavin Shaham[5], Robert O. Messing[6], Esther Visser[7], Michel C. van den Oever[7], Lovisa Holm[1], Estelle Barbier[1], Eric Augier[1], Markus Heilig[1‡]

Alcohol intake remains controlled in a majority of users but becomes "compulsive," i.e., continues despite adverse consequences, in a minority who develop alcohol addiction. Here, using a footshock-punished alcohol self-administration procedure, we screened a large population of outbred rats to identify those showing compulsivity operationalized as punishment-resistant self-administration. Using unsupervised clustering, we found that this behavior emerged as a stable trait in a subpopulation of rats and was associated with activity of a brain network that included central nucleus of the amygdala (CeA). Activity of PKCδ$^+$ inhibitory neurons in the lateral subdivision of CeA (CeL) accounted for ~75% of variance in punishment-resistant alcohol taking. Activity-dependent tagging, followed by chemogenetic inhibition of neurons activated during punishment-resistant self-administration, suppressed alcohol taking, as did a virally mediated shRNA knockdown of PKCδ in CeA. These findings identify a previously unknown mechanism for a core element of alcohol addiction and point to a novel candidate therapeutic target.

INTRODUCTION

Treatment of alcohol addiction, a major cause of morbidity and mortality globally, remains challenging (*1*). Despite major advances in the neuroscience of addiction, developing novel, mechanistically based treatments has proven elusive (*2*). Addiction develops only in a vulnerable minority of substance users (*3*), suggesting that research to discover novel treatments should consider individual differences in vulnerability for clinically relevant behaviors (*4*–*6*). Recently, we identified a neurobiological mechanism that contributes to individual vulnerability for one of these behaviors—choice of alcohol over a natural reward (*5*). We reported that pathological alcohol choice was found in a vulnerable minority of outbred rats and was the result of impaired γ-aminobutyric acid (GABA) clearance within the central nucleus of the amygdala (CeA) due to decreased expression of the GABA transporter GAT-3. Low GAT-3 expression within CeA was also found in postmortem brain tissue from patients with alcohol addiction. These findings converged with previous reports implicating increased GABA transmission within CeA in alcohol addiction (*7*, *8*). The involvement of CeA identified through these studies is also consistent with a recent human brain imaging–based analysis of networks involved in alcohol addiction (*9*).

Another hallmark of addictive disorders is substance use that continues despite adverse consequences, frequently called "compulsive use" (*10*). Alcohol is consumed by most people in many parts of the world, but only a subset of users transition to compulsive drinking (*3*, *11*). Compulsivity can be assessed under experimental conditions that appear to have translational validity, using as a proxy alcohol seeking that is resistant to punishment. For instance, a recent functional magnetic resonance imaging study allowed participants to work for alcohol, either when this was safe or under a high probability of punishment in the form of a mild electric shock. In the punished condition, light social drinkers markedly reduced or stopped their button pressing for alcohol, but heavy drinkers did not. Punishment-resistant button pressing for alcohol correlated with participant scores on the clinically validated Obsessive-Compulsive Drinking Scale (*12*) and was associated with increased connectivity between the anterior insula and the nucleus accumbens [NAc; (*13*)]. These findings parallel data in rats, where activity of an insula-NAc pathway has been shown to promote alcohol self-administration that is resistant to footshock punishment (*14*).

Although this and other animal studies have begun to identify mechanisms behind compulsive alcohol taking (*14*–*18*), the neural basis of individual differences in this behavior remain poorly understood. Here, we used a footshock-punished alcohol self-administration procedure (*5*, *14*) to identify neural and molecular substrates of individual differences in vulnerability for compulsive alcohol self-administration. We screened a large population of outbred rats and applied unsupervised clustering to identify those in which compulsivity, operationalized as punishment-resistant self-administration, emerged as a stable trait. To identify brain areas involved in compulsive alcohol self-administration, we carried out an extensive mapping using the neuronal activity marker Fos. Activity within a population of protein kinase Cδ–positive (PKCδ$^+$) inhibitory neurons in the lateral subdivision of CeA (CeL) (*19*) accounted for >70% of variance in punishment-resistant alcohol taking. Tagging and chemogenetically controlling the activity of CeL neurons active during punishment-resistant alcohol self-administration allowed us to examine their causal role in this behavior, while a short hairpin RNA (shRNA)–mediated knockdown allowed us to probe the causal role of PKCδ.

[1]Center for Social and Affective Neuroscience, BKV, Linköping University, Linköping 581 85, Sweden. [2]Psychosomatic Medicine Center, Sichuan Provincial People's Hospital, University of Electronic Science and Technology of China, Chengdu, China. [3]Centre for Discovery Brain Sciences, University of Edinburgh, 1 George Square, Edinburgh EH8 9JZ, UK. [4]Department of Anatomy and Neurobiology, University of Maryland School of Medicine, Baltimore, MD 21201, USA. [5]Behavioral Neuroscience Branch Intramural Research Program, National Institute on Drug Abuse (NIDA), NIH, Baltimore, MD 21224, USA. [6]Waggoner Center for Alcohol and Addiction Research and Departments of Neuroscience and Neurology, University of Texas at Austin, Austin, TX 78712, USA. [7]Department of Molecular and Cellular Neurobiology, Center for Neurogenomics and Cognitive Research, Amsterdam Neuroscience, Vrije Universiteit Amsterdam, 1081 HV Amsterdam, Netherlands.
*Corresponding author. Email: esi.domi@liu.se
†These authors contributed equally to this work.
‡Present address: Department of Psychiatry, Linköping University Hospital, Linköping, Sweden.

RESULTS

Punishment-resistant alcohol self-administration emerges in a minority of outbred rats

We screened multiple cohorts of outbred Wistar rats to assess individual differences in vulnerability for punishment-resistant alcohol self-administration (total: $n = 301$; for individual experiments and individual data points, see figs. S1 and S2). Rats were first trained to self-administer 20% alcohol for 12 weeks in the absence of punishment until they reached stable response rates on a fixed ratio 2 (FR2) reinforcement schedule (*20*). Under these unpunished conditions, alcohol self-administration rates were unimodally distributed (fig. S3A). We then assessed self-administration of alcohol when its delivery was punished with an electric footshock. When alcohol delivery was paired with a 0.2-mA, 0.5-s shock (but not 0.1 mA), alcohol self-administration was decreased on average (fig. S3B) as seen previously (*5*), but considerable individual differences were seen.

To classify rats into punishment resistant or sensitive, we calculated for each rat a resistance score [calculated as (punished alcohol deliveries)/(punished alcohol deliveries + mean alcohol deliveries of the last 3 nonpunished sessions); see (*21*)], obtained over 14 self-administration sessions under a 0.2-mA shock punishment (see Materials and Methods; Fig. 1A), and examined its distribution in the population. Distribution was initially unimodal but became bimodal from session 6 onward (Fig. 1B; Hartigans' dip test $D = 0.04$, $P = 0.002$). Unsupervised clustering identified two subpopulations that responded differentially to punishment, wherein rats with a resistance score of >0.45 were classified as "punishment-resistant" ($n = 114$, 38%), while those with a score of <0.45 were classified as "punishment-sensitive" ($n = 187$, 62%) (Fig. 1D). The threshold was based on a conservative limit of the second peak, identified with Hartigans' test of unimodality ($\alpha = 0.001$); it corresponded to about 20% decrease from baseline, unpunished alcohol self-administration. Confirmatory analyses supported that this classification resulted in groups that robustly differed in their resistance scores [Fig. 1E; Friedman nonparametric analysis of variance (ANOVA), group effect: $N_{14,301} = 990$, $P < 0.001$]. Bimodal distribution of self-administration under punished conditions was stable across several cohorts (fig. S3C).

Bimodal distribution and the presence of punishment resistance in a subpopulation of rats were specific for alcohol. In contrast, saccharin self-administration showed a unimodal distribution and remained sensitive to punishment until the end of the 14-day procedure (Fig. 1C) despite markedly higher unpunished response rates for saccharin compared to those found for alcohol (fig. S4). Baseline rates of unpunished alcohol self-administration did not differ between rats that went on to become resistant or sensitive, as measured by the resistance score ($F_{1,299} = 0.23$, $P = 0.63$). This is in line with previous research showing that high alcohol intake under unpunished conditions does not predict punishment-resistant drinking (*22*). With oral self-administration, lever pressing could potentially be increased in a nonspecific manner without the reinforcer being consumed. We therefore examined blood alcohol concentrations (BACs) following punished self-administration sessions and found that these were robustly increased in punishment-resistant rats compared to those that were punishment sensitive (19 ± 3.4 versus 3.6 ± 0.6 mg/dl; $t_{20} = 4.7$; $P < 0.001$). We also found a significant correlation between BAC and the resistance score ($r^2 = 0.52$, $P < 0.001$) (fig. S5A). Punishment-resistant and punishment-sensitive rats did not differ in shock sensitivity, and punishment sensitivity was not related to locomotor activity in a novel environment (fig. S5, B and D). In contrast, punishment-resistant rats showed a higher motivation to obtain alcohol than sensitive rats, as shown by elevated break points in a progressive-ratio reinforcement schedule (Fig. 1F; $t_{17} = 3.4$; $P < 0.01$) (*23*).

Punishment resistance is a stable individual trait and generalizes across models

Punishment resistance and sensitivity were preserved when punishment was reintroduced after allowing rats to reestablish unpunished alcohol self-administration (Fig. 1G; Friedman nonparametric ANOVA, group effect: $N_{6,16} = 13.29$, $P < 0.05$). This observation supports the notion that they are stable individual traits and parallels previous observations that compulsive alcohol seeking is maintained after prolonged periods of time (*24*). Punishment-resistant rats were also less sensitive to decreasing their alcohol intake when alcohol was adulterated with quinine (Fig. 1H; group: $F_{1,14} = 4.58$, $P = 0.05$, $\eta^2 = 0.24$; quinine concentration: $F_{6,84} = 18.34$, $P < 0.001$, $\eta^2 = 0.56$; group × quinine concentration: $F_{6,84} = 2.38$, $P < 0.05$, $\eta^2 = 0.14$). Post hoc analysis showed that resistance to quinine adulteration was higher in punishment-resistant than in punishment-sensitive rats at the higher quinine concentrations (150 and 200 mg/liter; $P < 0.05$). We also found a significant correlation between shock punishment and quinine resistance at 200 mg/liter ($r^2 = 0.14$, $P < 0.05$). Punishment-resistant and punishment-sensitive rats did not differ in quinine sensitivity per se (fig. S5E). Thus, aversion-resistant alcohol taking is a stable individual trait that generalizes across different experimental procedures commonly used to assess it (*14*).

A brain network associated with punishment resistance

Our next objective was to identify neural substrates of punishment-resistant alcohol self-administration. We carried out an activity mapping to identify cell populations activated during punished self-administration, as indexed by the immediate early gene Fos (*25*). Rats ($n = 62$) were screened for punishment resistance (resistant, $n = 21$; sensitive, $n = 41$); to control for activity merely driven by exposure to footshock, we also included an alcohol-naive yoked control group that received footshock but did not have access to self-administration ($n = 8$). Rats were perfused 90 min after the start of the last punished 30-min self-administration session (or after the onset of noncontingent shock exposure for the control group), and brains were collected for analysis of Fos immunoreactivity. We analyzed a set of brain regions thought to be involved in addiction (*26*), including prelimbic (PrL) and infralimbic (IL) medial prefrontal cortex (mPFC), orbitofrontal cortex (OFC), NAc shell (NAcSh) and core (NAcC), central amygdala (CeA), basolateral amygdala (BLA), periaqueductal gray (PAG), and paraventricular nucleus (PVN) and periventricular area (PVA) of the hypothalamus (fig. S6, A and B).

To identify networks associated with punishment resistance, we carried out a factor analysis of Fos-mapping data. To maximize variance, we analyzed data from punishment-resistant rats showing the least decrease from baseline ($n = 9$), punishment-sensitive rats showing the largest suppression of punished alcohol responding ($n = 9$), and yoked rats ($n = 8$). Activity in CeA, NAc, and PAG loaded on "network 1," which accounted for 37% of total variance in activity, while mPFC, OFC, and BLA loaded on "network 2," which accounted for 22% of variance (Fig. 2A; activity data and representative sections for individual brain structures are provided in fig. S6). Network 1 activity was higher in the punishment-resistant than in the punishment-sensitive group and correlated positively

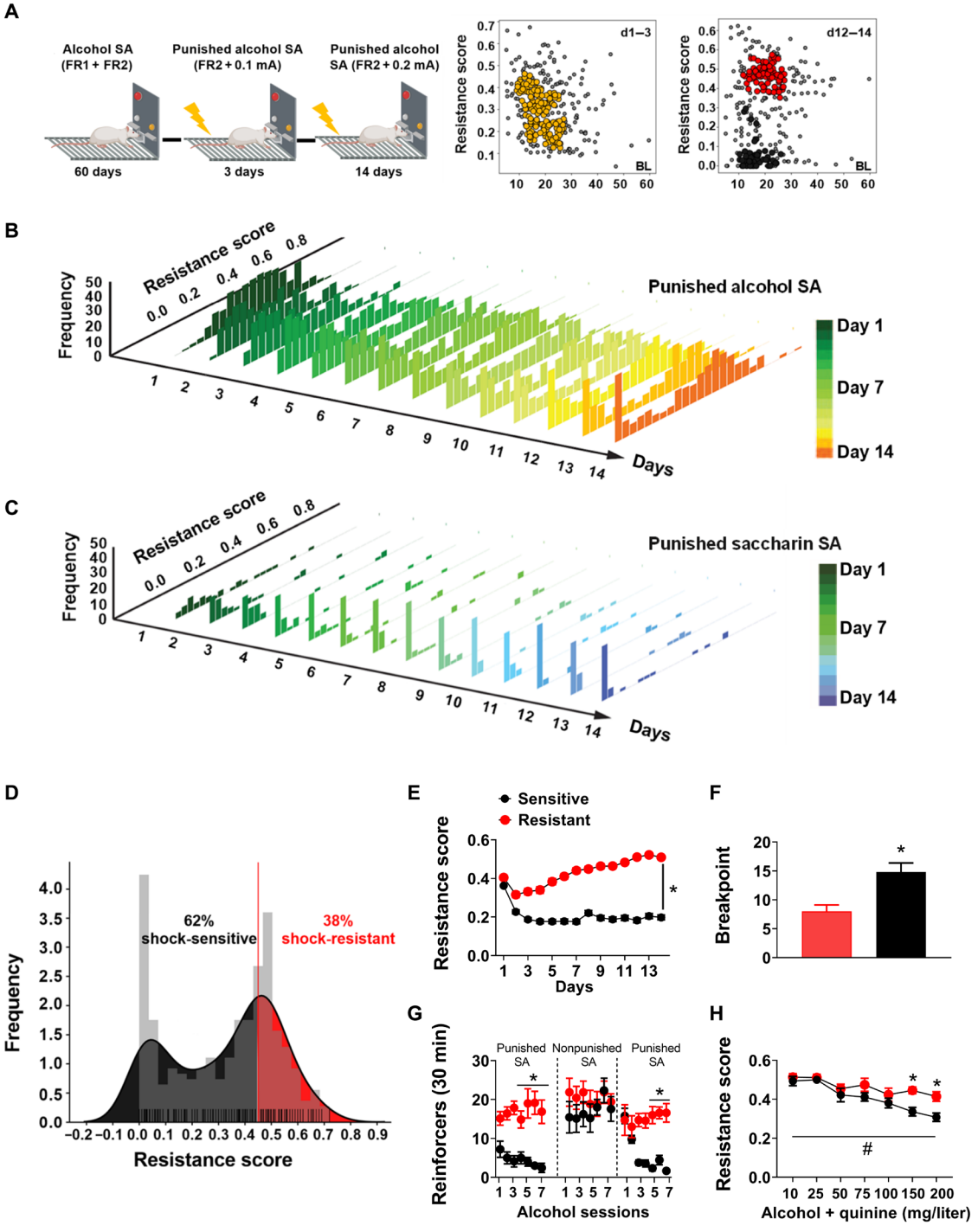

Fig. 1. Punishment-resistant alcohol self-administration emerges in a minority of outbred rats. (**A** and **B**) Schematic representation of the footshock punishment procedure and resistance score distribution of punished alcohol self-administration in the total cohort of outbred rats screened ($n = 301$) over 14 days (color-coded). Insets show individual distribution for days 1 to 3 and 12 to 14 of punished alcohol self-administration. (**C**) Resistance score distribution of punished saccharin self-administration across 14 days (color-coded). (**D**) Bimodal distribution of the population of punished alcohol self-administration; 38% ($n = 114$) of rats were punishment resistant, while 62% (187) were punishment sensitive. (**E**) Mean resistance score (±SEM) during a 30-min punished self-administration session of 20% EtOH (FR2). *$P < 0.001$. (**F**) Mean break points (±SEM) reached during a progressive ratio session of 20% alcohol in punishment-resistant ($n = 10$) and punishment-sensitive ($n = 9$) rats. *$P < 0.01$. (**G**) Mean reinforcers (±SEM) earned during a 30-min self-administration session of punished 20% EtOH (FR2) and unpunished alcohol self-administration in punishment-resistant ($n = 7$) and punishment-sensitive ($n = 9$) rats. Punishment-resistant rats obtained a significantly higher number of punished alcohol reinforcers during the last 3 days of baseline punished self-administration (left, *$P < 0.01$) and when footshock punishment was reintroduced. *$P < 0.001$. (**H**) Aversion-resistant alcohol drinking in punishment-resistant ($n = 7$) and punishment-sensitive rats ($n = 9$), shown by resistance to quinine adulteration of the alcohol solution (resistance score ± SEM for quinine-adulterated alcohol drinking, $^{\#}P < 0.001$, *$P < 0.05$). SA, self-administration; FR, fixed ratio; d, day; BL, baseline.

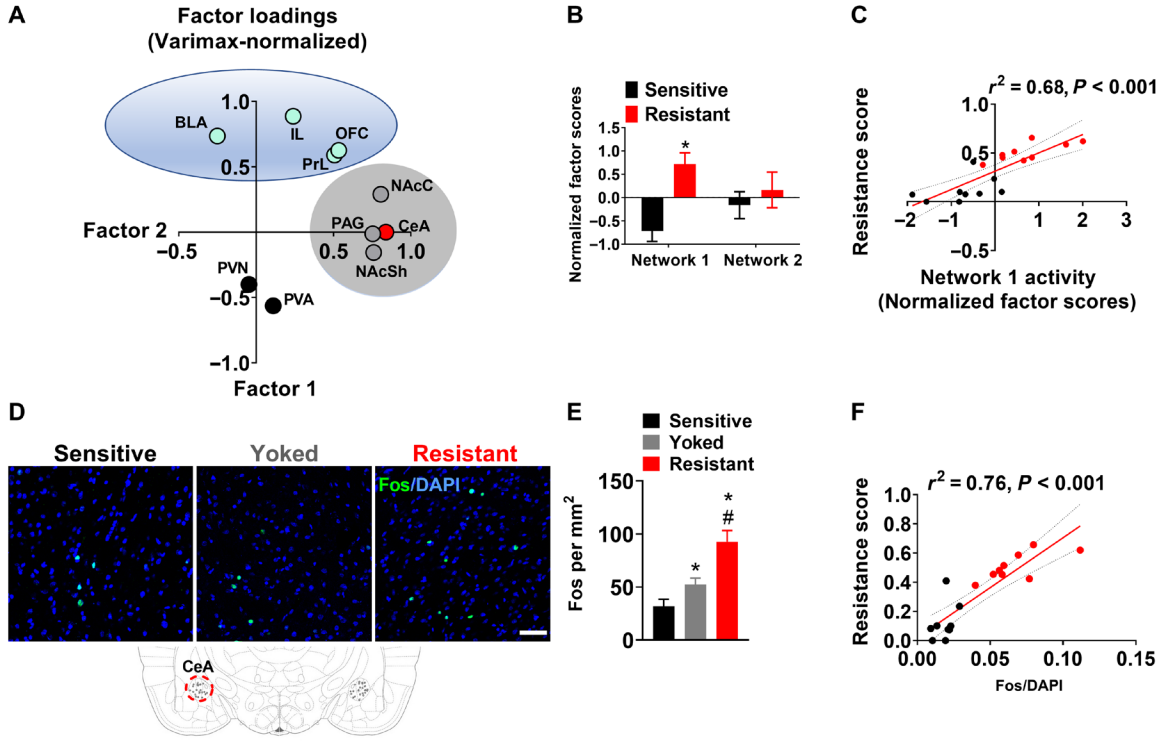

Fig. 2. A brain network associated with punishment resistance. (**A**) Factor analysis using principal component extraction followed by varimax normalized rotation of Fos immunoreactivity data identified two networks that showed highly correlated within-network activity. Network 1 consisted of CeA, PAG, NAcC, and NAcSh; network 2 consisted of OFC, PrL, IL, and BLA. (**B** and **C**) Activity of network 1, but not network 2, was increased in punishment-resistant rats (*$P < 0.001$) and correlated with punishment-resistant self-administration. (**D**) Representative images of Fos immunohistochemistry in CeA in shock-resistant and shock-sensitive rats. Scale bar, 50 μm. (**E**) Mean number of Fos-immunoreactive neurons/mm^2 (±SEM) in shock-resistant ($n = 9$), shock-sensitive ($n = 9$), and yoked rats ($n = 8$). *$P < 0.001$ versus the punishment-sensitive group; $^{\#}P < 0.001$ versus the yoked group. (**F**) Activity of CeA was particularly highly correlated with the resistance score. CeA, central nucleus of amygdala; PAG, periaqueductal gray; NAcC, nucleus accumbens core; NAcSh, NAc shell; OFC, orbitofrontal cortex; PrL, prelimbic cortex; IL, infralimbic cortex; BLA, basolateral amygdala.

with the resistance scores (Fig. 2, B and C; group: $F_{1,16} = 19.26$, $P < 0.001$, $\eta^2 = 0.55$, $r^2 = 0.68$, $P < 0.001$). Within network 1, Fos activity in CeA was higher in the resistant rats (Fig. 2, D and E; group: $F_{2,23} = 26.2$, $P < 0.001$, $\eta^2 = 0.69$; post hoc: $P < 0.001$; resistant versus both sensitive and yoked) and showed particularly high correlation with punishment resistance, accounting for 76% of variance in behavior (Fig. 2F; $r^2 = 0.76$, $P < 0.001$).

In contrast, activity within network 2 did not differ between punishment-resistant and punishment-sensitive rats (fig. S6C). Activity of PVA and PVN did not load onto either of the networks and also did not differ between punishment-resistant and punishment-sensitive rats. This lack of differential activity in structures mediating neuroendocrine responses to stress (i.e., PVN and PVA) was paralleled by a lack of group difference in corticosterone levels (fig. S5C).

Activity of CeA ensembles is necessary for punishment-resistant self-administration

We next examined whether neuronal activity in CeA plays a causal role in punishment resistance. To address this, we used a viral-mediated targeted recombination in active population (TRAP) approach (*27*, *28*) and selectively tagged ensembles of CeA neurons that were active during punished alcohol self-administration.

Rats ($n = 64$) were screened for punishment resistance, and unsupervised clustering identified punishment-resistant ($n = 23$) and shock-sensitive rats ($n = 41$). All resistant rats were used for tagging CeA ensembles, and sensitive rats ($n = 18$) were used for control experiments. Rats received CeA injections of a mixture containing two vectors: One was always AAV-Fos:CreER^{T2}, and the other was either a Cre-dependent hM4Di-mCherry or an mCherry control vector (fig. S7A). After viral vector surgeries, animals were returned to their home cage, and 3 weeks were allowed for vectors to express, as previously described (*29*). Rats then underwent 5 days of daily punished alcohol self-administration followed by systemic 4-hydroxytamoxifen (4TM) injections [2 hours after starting the last punishment session, as previously described (*27*, *29*, *30*)]. Another 3 weeks were then allowed for selective expression of the hM4Di DREADD in CeA neurons activated during punished self-administration. After five additional days of daily punished alcohol self-administration sessions, punishment-resistant rats expressing hM4Di-mCherry or the mCherry control vector received clozapine *N*-oxide (CNO), the synthetic ligand for hM4Di. To maximize specificity, CNO was microinjected directly into the CeA [1 mM per 0.3 μl per side as described (*31*)] 15 min before the punishment session (Fig. 3, A to C).

CNO injections decreased neuronal activity in CeA associated with punishment-resistant alcohol self-administration, as shown by the total number of activated (Fos-expressing) CeA neurons and double-labeled neurons positive for both Fos and mCherry, without affecting the number of mCherry-positive neurons neither in control nor in hM4Di-expressing rats (Fig. 3, D and E; $t_{15} = 5.6$, $P < 0.001$; $t_{15} = 2.2$, $P < 0.05$; $t_{15} = 1.5$, $P = 0.17$). This was accompanied by a

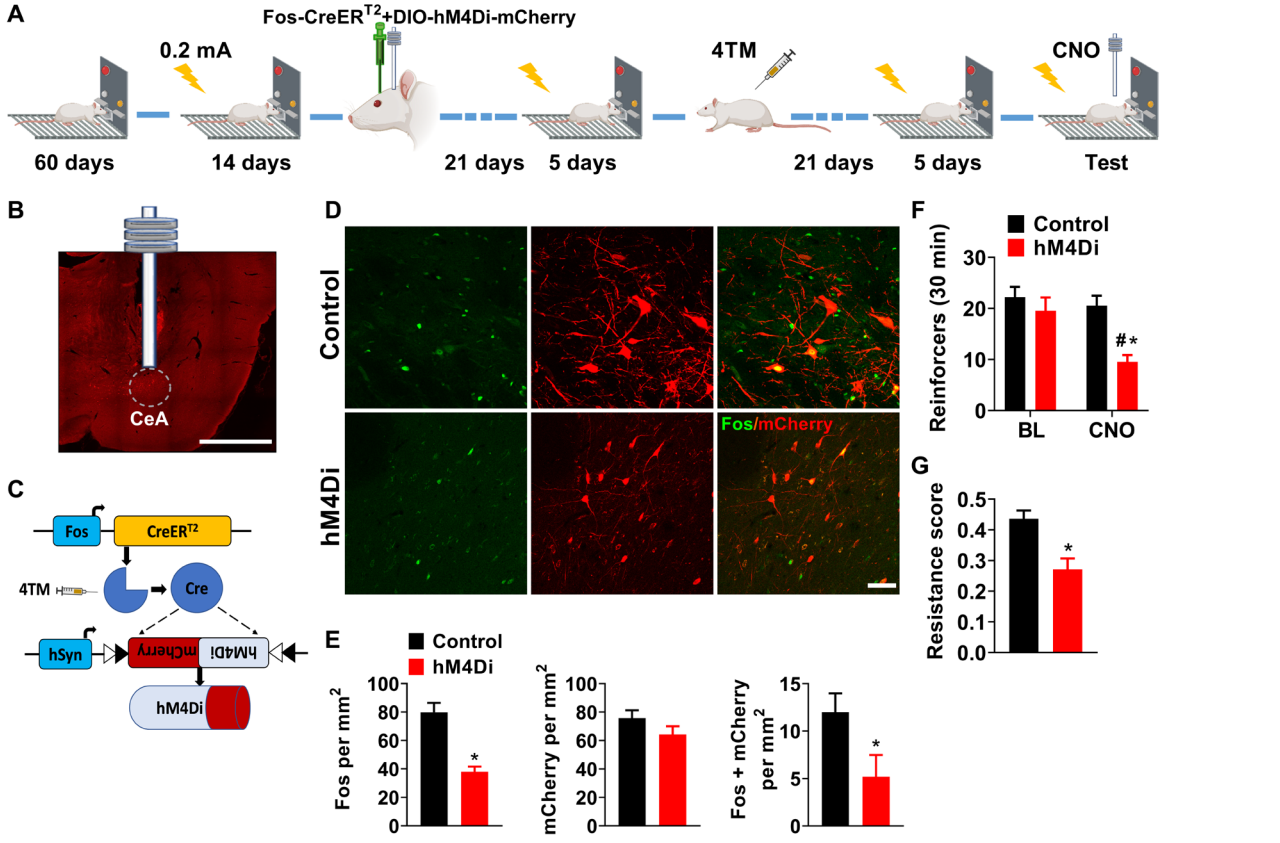

Fig. 3. Activity of CeA ensembles is necessary for punishment-resistant self-administration. (**A**) Schematic overview of the experimental design. (**B**) Virus injection site and cannula placement (scale bar, 2 mm). (**C**) Schematic representation of the TRAP approach. (**D** and **E**) Representative images of CeA photomicrographs showing Fos immunoreactivity (green) and mCherry colabeling in control ($n = 8$) and hM4Di ($n = 9$). Scale bar, 50 μm. Mean number of Fos-immunoreactive neurons (±SEM), mean number of mCherry immunoreactive neurons (±SEM), and mean number of Fos$^+$ mCherry-immunoreactive double-labeled neurons/mm^2. *$P < 0.001$, *$P < 0.05$. (**F**) Mean number of alcohol-reinforced lever presses (±SEM) during the 30-min test in control ($n = 11$) and hM4Di ($n = 12$) punishment-resistant CNO injected rats. *$P < 0.001$, $^{\#}P < 0.01$. (**G**) Mean resistance score (±SEM). *$P < 0.01$. BL, baseline; 4TM, 4-hydroxytamoxifen; CNO, clozapine *N*-oxide.

decrease in punishment-resistant self-administration (Fig. 3F; vector type: $F_{1,21} = 5.2$, $P < 0.05$, $\eta^2 = 0.2$; punishment condition: $F_{1,21} = 34.6$, $P < 0.001$, $\eta^2 = 0.62$; vector type × punishment condition: $F_{1,21} = 12.9$, $P < 0.001$, $\eta^2 = 0.38$). Post hoc analyses showed that alcohol self-administration was lower in punishment-resistant rats expressing hM4Di than in mCherry controls ($P < 0.001$) and their own baseline ($P < 0.01$). Resistance scores were also lower in hM4Di-expressing rats (0.27 ± 0.03) than in controls (0.43 ± 0.02) (Fig. 3G). Behavioral specificity of the chemogenetic manipulation was supported by a lack of CNO effect in mCherry controls and a lack of effect on general locomotor activity (fig. S10A). Thus, activity of neuronal ensembles within CeA promotes punishment-resistant alcohol self-administration.

To assess whether neurons that comprise these ensembles are local or project to targets outside the CeA, we visualized their main axonal projections. The AAV5 serotype hijacks the anterograde axonal transport system leading to mCherry expression in brain areas that receive projections from CeA neurons that were active during punished alcohol self-administration. Only direct monosynaptic targets of these neurons are expected to be labeled, as previous tracing experiments did not find transsynaptic transduction with this AAV serotype (*32*). Using this approach, we found that neuronal ensembles tagged in an activity-dependent manner during punishment-resistant alcohol self-administration were composed of both intrinsic and projecting neurons. Specifically, we identified local inputs to the CeM, as well as monosynaptic projections to the bed nucleus of stria terminalis (BNST) and the ventrolateral subdivision of the PAG (vlPAG) (fig. S8).

Punishment resistance is driven by activity of PKCδ$^+$ inhibitory neurons in CeA

CeA function relies on complex local microcircuits, which are, in part, defined by neurochemically identified neuronal populations (*33*). Our next objective was to examine whether CeA neurons that promote punishment-resistant alcohol self-administration map onto one of these populations. We carried out double-labeling immunohistochemistry to identify activated (Fos-positive) cells that also expressed PKCδ or somatostatin (SOM). These markers label two largely nonoverlapping populations of GABAergic cells that together constitute most CeA neurons (*34*). Opposing functions of PKCδ and SOM cells in the CeA have previously been shown in conditioned fear, pain modulation, appetitive behaviors, and addiction-related behaviors (*35*–*39*).

Within the CeL, Fos expression associated with punishment-resistant alcohol self-administration was exclusively colocalized with PKCδ labeling (Fig. 4A) and did not label SOM$^+$ neurons (fig. S9A). The number of cells positive for Fos and PKCδ and double-labeled

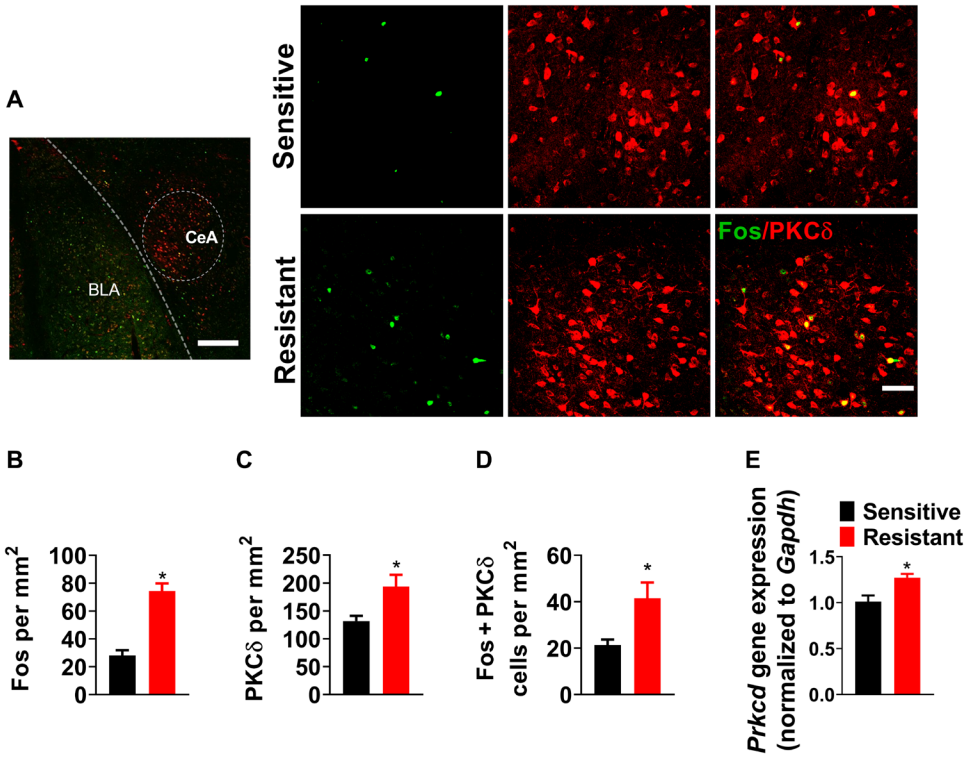

Fig. 4. Punishment resistance is driven by activity of PKCδ$^+$ inhibitory neurons in CeA. (**A**) Representative images of CeA photomicrographs showing Fos (green) and PKCδ (red) immunoreactivity colabeling [scale bars, 200 μm (left) and 50 μm (right)] in punishment-resistant ($n = 10$) and punishment-sensitive ($n = 9$) rats. (**B** to **D**) Mean number of cells (±SEM) positive for Fos, PKCδ, and double-labeled cells/mm^2. *$P < 0.001$, *$P < 0.05$, *$P < 0.01$. (**E**) Mean fold change in *Prkcd* mRNA levels in punishment-resistant ($n = 8$) and punishment-sensitive ($n = 6$) rats, measured by qPCR. *$P < 0.01$.

for both markers was significantly increased in CeL in punishment-resistant versus punishment-sensitive rats (Fig. 4, B to D; $t_{16} = 4.72$, $P < 0.001$; $t_{16} = 2.87$, $P < 0.05$; $t_{16} = 3.3$, $P < 0.01$). *Prkcd* mRNA was also higher in punishment-resistant rats (Fig. 4E; $t_{12} = 3.4$, $P < 0.01$). Last, the number of cells double-positive for Fos and PKCδ was significantly higher in the CeL of punishment-resistant rats than yoked control (fig. S9B), showing that increased Fos in PKCδ-expressing neurons is not merely due to shock exposure.

Thus, punishment-resistant alcohol self-administration is specifically associated with activity of PKCδ-expressing GABAergic CeL neurons. This population overlaps with cells that have been called "CeL-off" neurons, because they can gate behavioral responses to aversive stimuli through inhibition of centromedial (CeM) CeA outputs to the brainstem (*33*); for instance, silencing PKCδ-expressing CeL neurons increases conditioned freezing (*36*).

A mechanistic role of CeA-PKCδ in punishment-resistant alcohol self-administration

PKCδ has been used as a phenotypic marker to identify CeL-off cells, but is also of functional interest itself, as it is an intracellular signaling enzyme (*40*) and is involved in both alcohol potentiation of tonic GABA currents (*41*) and activation of adenylyl cyclase 7, which can, in turn, drive Fos induction (*42*). Elevated PKCδ expression in CeL of punishment-resistant rats suggests the possibility that up-regulated PKCδ signaling contributes to punishment resistance (*39*).

To examine this possibility, we knocked down PKCδ expression in CeA using an shRNA (*39*) and examined the consequences for punishment resistance. To maximize power, we established a stable baseline of punished alcohol self-administration in a cohort of 124 rats and then selected for the viral manipulation punishment-resistant rats showing the least decrease from baseline ($n = 37$) and punishment-sensitive rats showing the largest suppression of punished alcohol responding ($n = 38$). The remaining 49 rats were sacrificed. Punishment-resistant and punishment-sensitive rats were injected into CeA with an shRNA AAV vector targeting PKCδ or a scrambled control vector (Fig. 5A and fig. S7B). We validated viral expression in the CeA and confirmed that the knockdown was successful using both RNAscope in situ hybridization and quantitative polymerase chain reaction (qPCR) (Fig. 5, B and C; Mann-Whitney *U* test, $U = 11$, $P < 0.05$; $U = 9$, $P < 0.05$).

PKCδ knockdown significantly decreased both PKCδ and Fos expression associated with punished alcohol self-administration and the number of double-labeled cells (Fig. 5D; Fos group: $F_{1,18} = 26.2$, $P < 0.001$, $\eta^2 = 0.59$; knockdown: $F_{1,18} = 13.76$, $P < 0.001$, $\eta^2 = 0.43$; PKCδ group: $F_{1,18} = 24.7$, $P < 0.001$, $\eta^2 = 0.57$; knockdown: $F_{1,18} = 6.2$, $P < 0.05$, $\eta^2 = 0.25$; Fos$^+$ + PKCδ$^+$ group: $F_{1,18} = 44.5$, $P < 0.001$, $\eta^2 = 0.71$; knockdown: $F_{1,18} = 11.03$, $P < 0.01$, $\eta^2 = 0.37$). Decreased PKCδ expression resulted in decreased punishment-resistant alcohol self-administration (Fig. 5E; Friedman nonparametric ANOVA, group: $N_{5,75} = 170.4$, $P < 0.001$); post hoc comparisons showed that punishment-resistant PKCδ knockdown rats obtained fewer punished

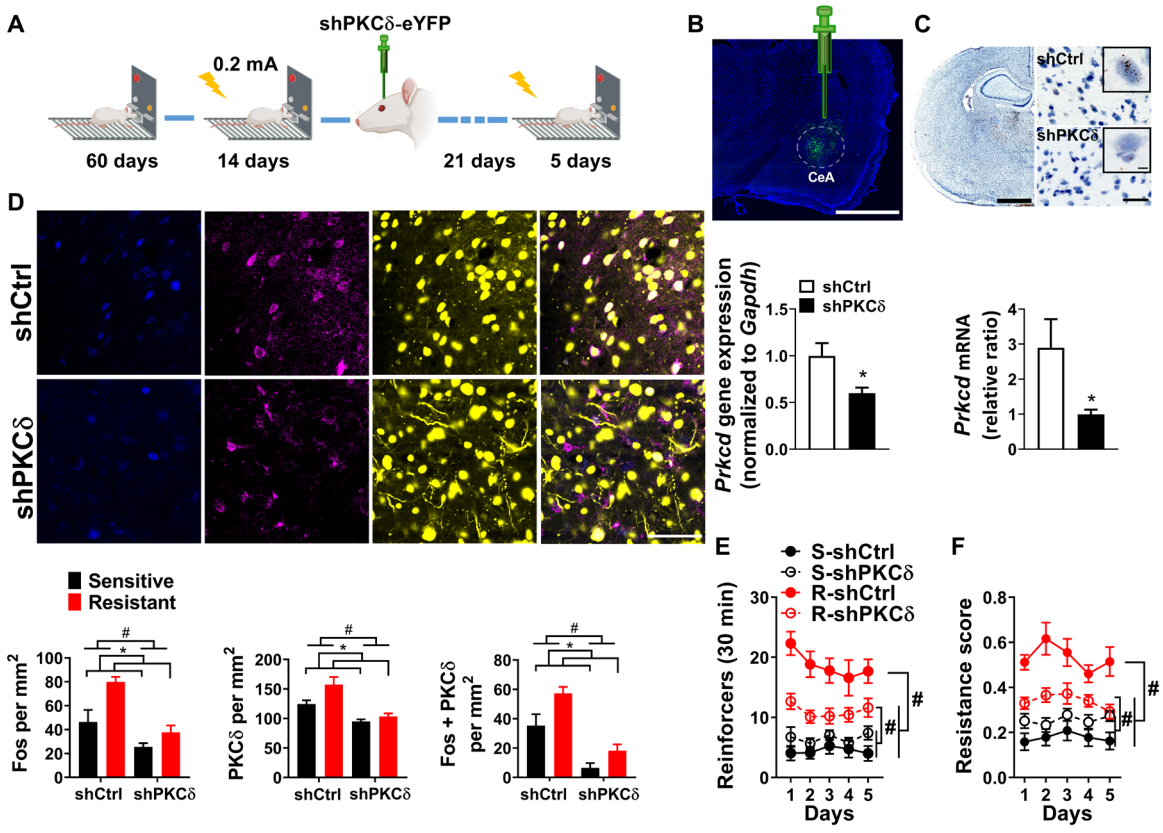

Fig. 5. A mechanistic role of CeA-PKCδ in punishment-resistant alcohol self-administration. (**A**) Experimental design. (**B**) Virus injection site (scale bar, 2 mm) and mean fold change in *Prkcd* mRNA levels following a viral-mediated knockdown ($n = 8$ per group). *$P < 0.05$. (**C**) Expression of *Prkcd* in the CeA measured by RNAscope. Brown dots represent the expression of *Prkcd* [scale bars, 2 mm (left), 50 μm (right), and 5 μm (inset)] ($n = 8$ per group). *$P < 0.05$. (**D**) Representative images of CeA photomicrographs (scale bar, 50 μm) showing Fos (blue), PKCδ (magenta) immunoreactivity, and yellow fluorescent protein (YFP) colabeling. Mean number of cells positive (±SEM) for Fos, PKCδ, and double-labeled cells in punishment-resistant ($n = 6$ per group) and punishment-sensitive ($n = 5$ per group) rats/mm^2. #$P < 0.001$, *$P < 0.001$, *$P < 0.05$, *$P < 0.01$. (**E**) Mean number of alcohol-reinforced lever presses (±SEM) during the 30-min punishment session control in punishment-resistant ($n = 19$) and punishment-sensitive rats ($n = 19$) receiving shCtrl, or shRNA knockdown of PKCδ ($n = 18$; $n = 19$). #$P < 0.001$. (**F**) Mean resistance score (±SEM). #$P < 0.001$.

reinforcers than scrambled punishment-resistant controls ($P < 0.001$). PKCδ knockdown also selectively decreased the resistance score in punishment-resistant rats (Fig. 5F; group × treatment: $F_{1,71} = 18.3$, $P < 0.001$, $\eta^2 = 0.2$); post hoc comparisons showed that resistance scores were significantly lower in punishment-resistant rats with a PKCδ knockdown than scrambled controls ($P < 0.001$). PKCδ knockdown did not affect control behaviors (fig. S10B). Thus, PKCδ-mediated signaling in CeL promotes punishment-resistant, compulsive-like alcohol self-administration.

DISCUSSION

To search for neural substrates of individual differences in compulsive alcohol use, we studied footshock-punished alcohol self-administration in outbred rats. The population distribution of punished responding for alcohol was initially unimodal but became bimodal over time. Ultimately, about one-third of rats showed resistance to punishment. This was specific for alcohol self-administration, while saccharin self-administration remained unimodally distributed and sensitive to punishment. The emergence of punishment resistance was not the result of differences in alcohol exposure or sensitivity to shock and generalized to another model of aversion resistance—quinine adulteration. These findings are in line with and extend previous reports (*14*, *21*). Our unsupervised clustering of punishment resistance over time in a large cohort of outbred rats indicates that this behavior is a stable individual trait and offers a model for studying its neural substrates. It is presently unknown whether emergence of punishment resistance in a subpopulation of rats reflects preexisting vulnerability or what has been referred to as "stochastic individuality" (*43*).

Alcohol addiction is a complex condition. A research domain criteria–based (*44*) view seeks to deconstruct it into functional domains that can be studied to identify underlying mechanisms and guide the development of mechanism-based, personalized treatments (*45*). In this framework, an impaired ability to control alcohol use despite negative consequences is one among several interacting susceptibility factors. Rather than operating in isolation, it is likely to promote the development and maintenance of alcohol addiction by interacting with factors such as incentive salience, negative reinforcement (*26*, *45*), choice of alcohol over natural rewards (*5*, *46*), lack of access to such rewards (*2*, *46*), or development of habits (*10*, *24*, *47*).

We found that activity in a network encompassing CeA, NAc, and PAG strongly correlated with punishment resistance. In contrast,

overall activity of network 2, which consisted of PFC, OFC, and BLA, did not correlate with this behavior. However, when regions were analyzed individually, we also found a robust increase of OFC neuronal activity in punishment-resistant rats. This is in agreement with previous work on the role of OFC in alcohol seeking and compulsive drug taking (*48*–*50*) and suggests that OFC activity may contribute to punishment-resistant alcohol self-administration.

Within network 1, Fos expression in the CeA accounted for ~75% of variance in punishment-resistant alcohol self-administration. Chemogenetic inhibition of activated CeA neurons selectively decreased this behavior, suggesting that putative ensembles of these neurons play a causal role in punishment resistance (*25*). These findings converge with previous observations implicating CeA in other alcohol addiction–related behaviors, including alcohol preference, withdrawal- or dependence-induced escalation of self-administration, and choice of alcohol over natural rewards (*5*, *7*, *8*, *51*, *52*).

Recently, the mPFC and insula have also been shown to play a role in punishment-resistant alcohol drinking through interactions with subcortical and brainstem connections (*14*, *17*, *53*). It is presently unknown how CeA interacts with these brain areas to produce punishment-resistant alcohol taking. However, a candidate node for this interaction is the PAG, which receives inputs from CeA, mPFC, and insula and modulates the balance between active and passive responses to aversive stimuli (*33*, *54*). A role for CeA-PAG interactions in punishment resistance would be consistent with a recently proposed role of CeA and its projections in negative urgency, i.e., acting rashly when in distress (*55*). It would also be in line with findings of a recent human brain imaging study, which identified the activity of a network connecting the OFC to subcortical regions, including the CeA and the brainstem as a correlate of alcohol use problems (*9*).

Both neurons intrinsic to CeA (*36*) and those projecting outside this structure were activated during punishment-resistant alcohol self-administration. Among the latter were neurons that showed direct monosynaptic connections with the BNST (*56*) and the ventrolateral column of the PAG (*57*). It is presently unknown how activity within inhibitory CeA microcircuits and its outputs, respectively, contributes to behavioral outcomes. For instance, depending on the intrinsic neuronal properties and topographic distribution, inhibitory CeA neurons target multiple PAG columns that, in turn, mediate different coping strategies in response to threat or stress (*57*, *58*).

Last, we found that CeA neurons promoting punishment-resistant alcohol taking were all PKCδ-expressing neurons in CeL. Although functional diversity has recently been suggested for these cells (*59*), a population of them can gate signaling from CeM outputs to their targets, including the PAG (*33*, *36*). Punishment-resistant rats showed increased Fos activity, specifically in PKCδ-expressing CeL neurons, and had also increased *Prkcd* expression. A possible interpretation of these findings is that PKCδ-expressing CeL neurons promote continued alcohol self-administration despite punishment because they inhibit CeA outputs that, in turn, mediate behavioral inhibition associated with aversive stimuli (*33*). The demonstration that a PKCδ knockdown in CeA decreased punishment-resistant alcohol intake additionally points to PKCδ-mediated signaling in this structure as a potential mechanism behind individual differences in vulnerability for compulsive alcohol taking. Because PKCδ is also expressed in the human CeA (*60*), this mechanism is potentially accessible for medications.

MATERIALS AND METHODS

Animals

Adult male Wistar rats (Charles River, Germany) weighing 225 to 250 g at the beginning of the experiments were used. Rats were pair-housed (except during the two-bottle free-choice drinking) in a temperature-controlled (21°C) and humidity-controlled environment with a reversed 12-hour light-dark cycle. Rats were given free access to chow and tap water for the duration of the experiment and were weighed at least once a week. All behavioral testing was conducted during the dark phase of the light-dark cycle. A detailed timeline of experimental training and testing can be found in fig. S1. The studies were conducted in accordance with the EU Directive 010/63/EU, as implemented in Swedish law, and was approved by the National Committee for Animal Research in Sweden and the Local Ethics Committee for Animal Care and Use at Linköping University.

Behavioral equipment

Operant training and testing were performed in 32 identical operant chambers (30.5 cm × 29.2 cm × 24.1 cm; Med Associates Inc., St. Albans, VT, USA) housed in sound-attenuating cubicles. Each operant chamber was equipped with two retractable levers positioned laterally to a liquid cup receptacle.

Alcohol self-administration

Operant- and drug-naive rats were trained to self-administer 20% (v/v) alcohol without sucrose/saccharin fading as described previously (*20*, *61*). Briefly, rats were first trained on an FR1 5s time-out (TO) schedule to self-administer 20% alcohol during 30-min sessions. The lever associated with alcohol was extended to mark the onset of the session and to signal alcohol availability. Pressing once was reinforced by the delivery of 100 μl of 20% alcohol in water in the adjacent drinking well and initiated a concomitant 5-s time-out period signaled by the illumination of the cue light above the lever. Responses during the TO period were recorded but had no programmed consequences. Sessions were conducted 5 days a week until self-administration rates stabilized, defined as a minimum of 20 sessions and no change greater than 15% in the total number of reinforcers earned during the last three sessions. Once a stable self-administration baseline was reached, the FR was increased and a minimum of 20 FR2 sessions were performed until stabilization of performance.

Footshock-punished alcohol self-administration

Alcohol taking despite adverse consequences was assessed as responding for alcohol when its delivery was associated with a footshock punishment. Briefly, conditions were identical to baseline self-administration (i.e., 30-min sessions), but each completed FR2 ratio (i.e., two responses) was paired with a footshock (0.1 to 0.2 mA, 0.5 s), contingent with the delivery of a volume of 100 μl of 20% alcohol in water in the adjacent drinking well. The resistance score was calculated as follows: (punished alcohol deliveries)/(punished alcohol deliveries + mean alcohol deliveries of the last three non-punished sessions) (*21*). Each rat in the yoked group received the same number of electric footshocks as a corresponding punishment-resistant rat. Saccharin self-administration was performed under the same conditions as for alcohol self-administration.

Footshock-punished saccharin self-administration

Briefly, rats were trained to self-administer 0.2% saccharin in 30-min sessions on an FR1 5s TO schedule of reinforcement. Once a stable

self-administration baseline was reached (a total of 15 FR2 sessions), the punished saccharin self-administration procedure was identical to alcohol self-administration.

Pain sensitivity

Animals were placed in the operant chamber, and footshock was delivered starting at 0.05 mA and increasing shock intensity by 0.05 mA every 30 s. Footshock threshold was defined as a jump with all four paws off the grid.

Progressive ratio schedule of reinforcement

The motivation to obtain alcohol was assessed using a progressive ratio schedule (*5*, *23*). Conditions were identical to baseline self-administration, except that the response requirement to receive a single alcohol reinforcer was increased within the session according to the following formula: 1, 2, 3, 4, 6, 8, 10, 12, 16, 20, 24, 28, 32 …. The self-administration session terminated once 30 min had elapsed without a reinforcer being obtained. The breakpoint was defined as the last completed response requirement during the progressive ratio test.

Quinine adulteration

Resistance to consuming alcohol despite adverse consequences was additionally assessed using quinine adulteration (*15*, *62*). Punishment-sensitive rats were allowed to recover their alcohol lever pressing after removing the footshock. Then, alcohol was mixed with increasing concentrations of quinine (10, 25, 50, 75, 100, 150, and 200 mg/liter) during FR2 alcohol self-administration for a minimum of three test sessions per quinine concentration to ensure stability of the behavior. Compulsive-like behavior was assessed as the resistance score in alcohol self-administration after addition of quinine: (quinine-adulterated alcohol deliveries)/(quinine-adulterated alcohol deliveries + mean alcohol deliveries of the last three baseline sessions).

Two-bottle free-choice drinking

As a control for taste reactivity to quinine, consumption of and preference for water and quinine were measured using a two-bottle free-choice continuous access (*63*). Previously grouped housed rats were single-housed during this experiment. Rats had access to one bottle of the test solution of quinine (5, 10, 25, and 50 mg/liter) and one bottle of water for 24 hours. Bottles were weighted every day at the same hour, and the position of the bottles was alternated to control for a potential side preference. Preference score for the test solution was calculated as follows: (volume of adulterated solution ingested)/(volume of adulterated solution + water).

Plasma corticosterone analysis

Blood samples were collected from the tail vein after rats were classified as punishment resistant and punishment sensitive. Samples were collected into heparin-coated tubes and centrifuged for 5 min at 2000*g* to separate the plasma. Plasma was transferred into new tubes and stored at −80°C until further analysis. Corticosterone was extracted by adding five parts of ethyl acetate (Thermo Fisher Scientific Inc., Waltham, MA, USA) to each plasma sample. The organic solvent layer was first transferred to a water-prefilled tube and then to a second tube. This procedure was repeated twice before the samples were dried in a vacuum concentrator. Samples were redissolved in assay buffer from the DetectX Corticosterone Enzyme Immunoassay Kit (Arbor Assays, Ann Arbor, MI, USA). Thereafter, the manufacturer's instructions were followed.

Blood alcohol concentration

Blood was collected from the lateral tail vein of punishment-resistant and punishment-sensitive rats immediately after the 30-min session. The colorimetric ethanol (EtOH) assay kit from Sigma-Aldrich (Stockholm, Sweden) was used according to the manufacturer's instructions to determine BAC.

Locomotor reactivity to novelty

Reactivity to novelty (*64*, *65*) was assessed using six identical standard locomotor activity testing chambers (44.5 cm × 44.5 cm × 30.5 cm; Med Associates Inc., St. Albans, VT, USA) housed in sound-attenuating cubicles during a single 30-min session. In accordance with a previous study (*65*), we classified rats within the upper quartile of locomotor activity (n = 7) as high responders, whereas the lower quartile (n = 8) was classified as low responders.

Surgery

All surgeries were performed after 14 days of punished alcohol self-administration. Animals were anesthetized with isoflurane (2 to 3%, Baxter) and injected with buprenorphine [0.03 mg/kg, subcutaneously (sc)] 30 min before surgery to relieve pain. Ketoprofen (5 mg/kg, sc) was injected after surgery and the following day to relieve pain and reduce inflammation. Animals were allowed to recover from surgery for 1 week and were then reexposed to the footshock punishment procedure 3 weeks later to allow the viral expression. We excluded a total of 13 rats because of cannula or injection misplacement.

Viral injections

For viral microinjections into the CeA, we used the following coordinates based on pilots referring to the rat brain atlas (*66*) and previous studies (*39*, *67*): antero-posterior (AP), −2.5 mm; medio-lateral (ML), ±4.5 mm; and dorso-ventral (DV), −8.5 mm. To knock down PKCδ expression, we injected either shPKCδ (scAAV$_1$-shPKCδ-CMV-IE-Nuc-eYFP; titer: 2.56×10^{12}) or shCtrl (scAAV$_1$-shCtrl-CMV-IE-Nuc-eYFP; titer: 3.24×10^{12}) bilaterally into CeA at a volume of 0.75 µl per side at a flow rate of 0.25 µl per min followed by an additional 5 min to allow diffusion as previously described (*39*).

For the viral-based TRAP approach, we used the following viral mixture: AAV$_5$-Fos:CreERT^2 (titer: 1.2×10^{13}), with either AAV$_5$-hSyn-DIO-hM4Di-mCherry (titer: 7.0×10^{12}; Addgene 44362) or AAV$_5$-hSyn-DIO-mCherry (titers: 5.0×10^{12} to 6.0×10^{12}; Addgene 50459). The viral mixture (AAV-Fos:CreERT^2 and Cre-dependent AAV; 1:500 ratio; AAV-Fos:CreERT^2; final titer of 2.4×10^{10}) was injected bilaterally into the CeA. Each side received 0.5 µl at a flow rate of 0.25 µl per minute followed by an additional 5 min to allow diffusion.

Cannula implantation

We implanted the guide cannulas (26 gauge; Plastics One) 2 mm above the CeA bilaterally using the following coordinates: AP, −2.5 mm; ML, ±4.5 mm; and DV, −6.4 mm. Cannulas were anchored to the skull with jeweler's screws and dental cement (Paladur, Agnthos).

4TM treatment

The 4TM treatment (H6278, Sigma-Aldrich) was dissolved as previously described (*29*, *68*). The final solution contained 4TM (2.5 mg/ml),

5% dimethyl sulfoxide, and 1% Tween 80 in saline. Animals received 4TM (25 mg/kg, intraperitoneally) 2 hours after the punishment session.

Chemogenetic inhibition

CNO (4936, TOCRIS) was dissolved in artificial cerebrospinal fluid (3525, TOCRIS) as previously described (*69*, *70*) at a concentration of 1 mM. Rats received 0.3 µl per side through the 33-gauge injectors (2 mm below the cannula placement) at a rate of 0.15 µl/min, 15 min before the punishment session.

RNA extraction and qPCR

Brains were rapidly removed, and amygdala samples were dissected from a 2-mm-thick coronal slice taken in a Kopf brain slicer, as previously described (*71*), and stored at −80°C. RNA was extracted using the RNeasy Plus Mini Kit (74136, Qiagen), following the manufacturer's instructions. Total RNA was reverse-transcribed into cDNA using the High-Capacity cDNA Reverse Transcription Kit (4368814, Life Technologies, Carlsbad, CA). The reactions were run on the Veriti 96-Well Fast Thermal Cycler (Life Technologies, Carlsbad, CA). Inventoried TaqMan gene expression assay probes (*Prkcd*: Rn00440891 and *Gapdh*: Rn4308313; Life Technologies, Carlsbad, CA) were used to assess the expression of the target gene on an ABI 7900HT Fast Real-time PCR system (Life Technologies, Carlsbad, CA). *Prkcd* expression was quantified by normalizing the data to the endogenous reference gene *Gapdh*, using RQ Manager 1.2 (Life Technologies, Carlsbad, CA) by calculating an RQ (relative quantification) value using $2^{-\Delta\Delta CT}$ analysis (*72*).

RNAscope in situ hybridization assay

Rats were sacrificed 1 day after completion of behavioral experiments. Brains were removed, flash-frozen, and stored at −80°C until further processing. After equilibration in a cryostat (CM 3050S) at −20°C for 2 hours, we collected 12-µm brain slices at approximately bregma −2.4 mm (*66*) and mounted the slices directly onto SuperFrost Plus slides (Thermo Fisher Scientific).

3,3'-Diaminobenzidine (DAB) in situ hybridization assay was performed using RNAscope 2.5 HD Detection Reagents-BROWN assay (catalog no. 322310, Advanced Cell Diagnostics), according to the user manual for fresh frozen tissue. Briefly, brain slices were fixed in 10% neutral-buffered formalin (Thermo Fisher Scientific) for 15 min at 4°C and dehydrated in 50, 70, 100, and 100% ethanol (EtOH). Brain slices were then treated with protease solution (pretreatment 4) at room temperature for 20 min. After three washes with 1× phosphate-buffered saline (PBS), brain slices were incubated with the target probe for *Prkcd* mRNA (catalog no. 441791, Advanced Cell Diagnostics; GeneBank accession number NM_011103.3) at 40°C for 2 hours in the HybEZ oven (Advanced Cell Diagnostics). Next, brain slices were incubated with preamplifier, amplifier, and labeled probes at 40°C (AMP1, AMP3, and AMP5 for 30 min; AMP2, AMP4, and AMP6 for 15 min). Sections were then incubated with DAB substrate at room temperature for 10 min to visualize the mRNA signal. After counterstaining with 50% hematoxylin followed by 0.02% ammonia water, sections were dehydrated in 70%, 95%, and, finally, 100% EtOH. Sections were merged in xylene solution (3 min) and coated with quick-hardening mounting medium (catalog no. 03989, Sigma-Aldrich) and covered with cover slides (Thermo Fisher Scientific).

Images of brain sections were acquired through a Leica Aperio CS2 digital pathology slide scanner. Aperio ImageScope software (v12.3) was used to analyze the images. Amygdala region was selected and magnified equally to 40× objective lens. We assume that each brown dot represents a single molecule of mRNA. Dark brown staining dots were counted using ImageJ software in a blinded manner. Results were reported as mRNA molecule per cells in a 0.04-mm^2-size window.

Fluorescent immunohistochemistry

Rats were anesthetized using isoflurane 90 min after the start of the footshock session (day 15) and transcardially perfused with 0.9% saline followed by 4% paraformaldehyde (PFA). Brains were removed and postfixed in 4% PFA for 2 hours and then transferred into 30% sucrose solution at 4°C until sinking. Coronal brain sections (20 µm) of the amygdala (AP bregma level of −1.92 to −2.92 mm) were collected using a Leica cryostat and stored in cryoprotectant (20% glycerol and 30% ethylene glycol in 0.1 M PBS) at −20°C until further processing.

To verify the viral injection site and cannula placement, we selected four series of sections from each rat, rinsed in PBS (3 × 10 min), and then mounted them onto SuperFrost Plus slides, air-dried, and cover-slipped with antifade mountant with 4′,6-diamidino-2-phenylindole (DAPI) (P36962, Invitrogen).

For Fos, PKCδ, and SOM immunofluorescence staining, floating brain sections were washed in PBS (3 × 10 min) and then blocked in a solution of 4% bovine serum albumin and 0.2% Triton X-100 dissolved in PBS for 1 hour at room temperature. For labeling Fos, PKCδ, and SOM, the following antibodies were used: rabbit anti-cFos [1:1000; ab190289, Research Resource Identifier (RRID): AB_2737414, Abcam], mouse anti-PKCδ (1:500; 610398, RRID: AB_397781, BD Biosciences), and mouse anti-SOM (1:100; GTX71935, RRID: AB_383280, GeneTex). Sections were incubated with primary antibodies overnight at 4°C. After rinsing in PBS three times, the sections were incubated for 2 hours at room temperature with the following secondary antibodies: goat anti-rabbit DyLight 405 (1:200; 35550, RRID: AB_1965945, Thermo Fisher Scientific), donkey anti-rabbit Alexa Fluor 488 (1:200; A-21206, RRID: AB_2535792, Thermo Fisher Scientific), goat anti-mouse Alexa Fluor 568 (1:200; A-11004, RRID: AB_2534072, Thermo Fisher Scientific), and goat anti-mouse Alexa Fluor 647 (1:200; A-21235, RRID: AB_2535804, Thermo Fisher Scientific). Sections were rinsed in PBS three times, mounted on slides, and cover-slipped with Antifade Mountant DAPI (P36962, Invitrogen) or the Antifade Mountant (P36961, Invitrogen).

Images for viral expression and cannula placement were acquired through a Leica DMi8 fluorescence microscope with a 10× objective lens. All Fos, PKCδ, and SOM immunofluorescence images were acquired through a Zeiss LSM 800 upright confocal microscope using a 20× objective lens. We quantified the total number of Fos-, PKCδ-, DAPI-, and mCherry-positive cells in CeA in a manner blinded to the experimental condition. For each rat, labeled cells were quantified from two hemispheres of three sections, and we averaged the counts to give a mean number of each immunoreactive cell type. All images were adjusted to match contrast and brightness in Fiji software; cells were identified by DAPI immunostaining.

Statistical analysis

Data were first examined for homogeneity of variances using Levene's test. When deviation from homogeneity of variances was detected, nonparametric analysis was used. Hartigans' dip test for unimodality (*73*) implemented in R (https://cran.r-project.org/web/packages/diptest/) and UniDip Python package was used to test

unimodality of one-dimensional distributions. Intervals were calculated with UniDip at the $\alpha = 0.05$ level. Unsupervised clustering was performed using the "Density-based spatial clustering of applications with noise" (DBSCAN) algorithm (*74*), as implemented in the scikit-learn (sklearn) Python package. DBSCAN clustering determines the number of clusters in an unsupervised manner. All other data were analyzed with STATISTICA, StatSoft 13.0 RRID: SCR_014213) using Student's *t* test or ANOVA, with factors for the respective analysis indicated in conjunction with its results. Post hoc analyses were conducted when appropriate using Newman-Keuls test. A factor analysis was performed using principal component extraction followed by normalized varimax rotation. Correlation analysis between resistance scores and Fos expression in the CeA were performed using the Pearson correlation value. The accepted level of significance for all tests was $P < 0.05$.

SUPPLEMENTARY MATERIALS

Supplementary material for this article is available at http://advances.sciencemag.org/cgi/content/full/7/34/eabg9045/DC1

View/request a protocol for this paper from *Bio-protocol*.

REFERENCES AND NOTES

1. A. F. Carvalho, M. Heilig, A. Perez, C. Probst, J. Rehm, Alcohol use disorders. *Lancet* **394**, 781–792 (2019).
2. M. Venniro, M. L. Banks, M. Heilig, D. H. Epstein, Y. Shaham, Improving translation of animal models of addiction and relapse by reverse translation. *Nat. Rev. Neurosci.* **21**, 625–643 (2020).
3. J. C. Anthony, Epidemiology of drug dependence, in *Neuropsychopharmacology: The Fifth Generation of Progress*, K. L. Davis, D. Charney, J. T. Coyle, C. Nemeroff, Eds. (Lippincott Williams and Wilkins, 2002), chap. 109, pp. 1557–1573.
4. V. Deroche-Gamonet, D. Belin, P. V. Piazza, Evidence for addiction-like behavior in the rat. *Science* **305**, 1014–1017 (2004).
5. E. Augier, E. Barbier, R. S. Dulman, V. Licheri, G. Augier, E. Domi, R. Barchiesi, S. Farris, D. Nätt, R. D. Mayfield, L. Adermark, M. Heilig, A molecular mechanism for choosing alcohol over an alternative reward. *Science* **360**, 1321–1326 (2018).
6. P. V. Piazza, V. Deroche-Gamonet, A multistep general theory of transition to addiction. *Psychopharmacology* **229**, 387–413 (2013).
7. M. Roberto, S. G. Madamba, D. G. Stouffer, L. H. Parsons, G. R. Siggins, Increased GABA release in the central amygdala of ethanol-dependent rats. *J. Neurosci.* **24**, 10159–10166 (2004).
8. N. W. Gilpin, M. A. Herman, M. Roberto, The central amygdala as an integrative hub for anxiety and alcohol use disorders. *Biol. Psychiatry* **77**, 859–869 (2015).
9. T. Jia, C. Xie, T. Banaschewski, G. J. Barker, A. L. W. Bokde, C. Büchel, E. B. Quinlan, S. Desrivières, H. Flor, A. Grigis, H. Garavan, P. Gowland, A. Heinz, B. Ittermann, J.-L. Martinot, M.-L. P. Martinot, F. Nees, D. P. Orfanos, L. Poustka, J. H. Fröhner, M. N. Smolka, H. Walter, R. Whelan, G. Schumann, T. W. Robbins, J. Feng; IMAGEN Consortium, Neural network involving medial orbitofrontal cortex and dorsal periaqueductal gray regulation in human alcohol abuse. *Sci. Adv.* **7**, eabd4074 (2021).
10. C. Lüscher, T. W. Robbins, B. J. Everitt, The transition to compulsion in addiction. *Nat. Rev. Neurosci.* **21**, 247–263 (2020).
11. B. F. Grant, R. B. Goldstein, T. D. Saha, S. P. Chou, J. Jung, H. Zhang, R. P. Pickering, W. J. Ruan, S. M. Smith, B. Huang, D. S. Hasin, Epidemiology of *DSM-5* alcohol use disorder: Results from the national epidemiologic survey on alcohol and related conditions III. *JAMA Psychiat.* **72**, 757–766 (2015).
12. R. F. Anton, D. H. Moak, P. K. Latham, The obsessive compulsive drinking scale: A new method of assessing outcome in alcoholism treatment studies. *Arch. Gen. Psychiatry* **53**, 225–231 (1996).
13. E. N. Grodin, L. Sussman, K. Sundby, G. M. Brennan, N. Diazgranados, M. Heilig, R. Momenan, Neural correlates of compulsive alcohol seeking in heavy drinkers. *Biol. Psychiatry Cogn. Neurosci. Neuroimaging* **3**, 1022–1031 (2018).
14. T. Seif, S.-J. Chang, J. A. Simms, S. L. Gibb, J. Dadgar, B. T. Chen, B. K. Harvey, D. Ron, R. O. Messing, A. Bonci, F. W. Hopf, Cortical activation of accumbens hyperpolarization-active NMDARs mediates aversion-resistant alcohol intake. *Nat. Neurosci.* **16**, 1094–1100 (2013).
15. J. Wolffgramm, An ethopharmacological approach to the development of drug addiction. *Neurosci. Biobehav. Rev.* **15**, 515–519 (1991).
16. F. W. Hopf, S.-J. Chang, D. R. Sparta, M. S. Bowers, A. Bonci, Motivation for alcohol becomes resistant to quinine adulteration after 3 to 4 months of intermittent alcohol self-administration. *Alcohol. Clin. Exp. Res.* **34**, 1565–1573 (2010).
17. C. A. Siciliano, H. Noamany, C.-J. Chang, A. R. Brown, X. Chen, D. Leible, J. J. Lee, J. Wang, A. N. Vernon, C. M. Vander Weele, E. Y. Kimchi, M. Heiman, K. M. Tye, A cortical-brainstem circuit predicts and governs compulsive alcohol drinking. *Science* **366**, 1008–1012 (2019).
18. K. S. Jadhav, P. J. Magistretti, O. Halfon, M. Augsburger, B. Boutrel, A preclinical model for identifying rats at risk of alcohol use disorder. *Sci. Rep.* **7**, 9454 (2017).
19. J. Gründemann, A. Lüthi, Ensemble coding in amygdala circuits for associative learning. *Curr. Opin. Neurobiol.* **35**, 200–206 (2015).
20. E. Augier, M. Flanigan, R. S. Dulman, A. Pincus, J. R. Schank, K. C. Rice, C. Kejun, M. Heilig, J. D. Tapocik, Wistar rats acquire and maintain self-administration of 20% ethanol without water deprivation, saccharin/sucrose fading, or extended access training. *Psychopharmacology* **231**, 4561–4568 (2014).
21. N. J. Marchant, E. J. Campbell, K. Kaganovsky, Punishment of alcohol-reinforced responding in alcohol preferring P rats reveals a bimodal population: Implications for models of compulsive drug seeking. *Prog. Neuropsychopharmacol. Biol. Psychiatry* **87**, 68–77 (2018).
22. V. Vengeliene, E. Celerier, L. Chaskiel, F. Penzo, R. Spanagel, RESEARCH FOCUS ON COMPULSIVE BEHAVIOUR IN ANIMALS: Compulsive alcohol drinking in rodents. *Addict. Biol.* **14**, 384–396 (2009).
23. W. Hodos, Progressive ratio as a measure of reward strength. *Science* **134**, 943–944 (1961).
24. C. Giuliano, Y. Peña-Oliver, C. R. Goodlett, R. N. Cardinal, T. W. Robbins, E. T. Bullmore, D. Belin, B. J. Everitt, Evidence for a long-lasting compulsive alcohol seeking phenotype in rats. *Neuropsychopharmacology* **43**, 728–738 (2018).
25. F. C. Cruz, E. Koya, D. H. Guez-Barber, J. M. Bossert, C. R. Lupica, Y. Shaham, B. T. Hope, New technologies for examining the role of neuronal ensembles in drug addiction and fear. *Nat. Rev. Neurosci.* **14**, 743–754 (2013).
26. G. F. Koob, N. D. Volkow, Neurocircuitry of addiction. *Neuropsychopharmacology* **35**, 217–238 (2010).
27. C. J. Guenthner, K. Miyamichi, H. H. Yang, H. C. Heller, L. Luo, Permanent genetic access to transiently active neurons via TRAP: Targeted recombination in active populations. *Neuron* **78**, 773–784 (2013).
28. E. Visser, M. R. Matos, R. J. van der Loo, N. J. Marchant, T. J. de Vries, A. B. Smit, M. C. van den Oever, A persistent alcohol cue memory trace drives relapse to alcohol seeking after prolonged abstinence. *Sci. Adv.* **6**, eaax7060 (2020).
29. M. R. Matos, E. Visser, I. Kramvis, R. J. van der Loo, T. Gebuis, R. Zalm, P. Rao-Ruiz, H. D. Mansvelder, A. B. Smit, M. C. van den Oever, Memory strength gates the involvement of a CREB-dependent cortical fear engram in remote memory. *Nat. Commun.* **10**, 2315 (2019).
30. G. Giannotti, J. A. Heinsbroek, A. J. Yue, K. Deisseroth, J. Peters, Prefrontal cortex neuronal ensembles encoding fear drive fear expression during long-term memory retrieval. *Sci. Rep.* **9**, 10709 (2019).
31. M. Venniro, D. Caprioli, M. Zhang, L. R. Whitaker, S. Zhang, B. L. Warren, C. Cifani, N. J. Marchant, O. Yizhar, J. M. Bossert, C. Chiamulera, M. Morales, Y. Shaham, The anterior insular cortex→central amygdala glutamatergic pathway is critical to relapse after contingency management. *Neuron* **96**, 414–427.e8 (2017).
32. B. Zingg, X.-l. Chou, Z.-g. Zhang, L. Mesik, F. Liang, H. W. Tao, L. I. Zhang, AAV-mediated anterograde transsynaptic tagging: Mapping corticocollicular input-defined neural pathways for defense behaviors. *Neuron* **93**, 33–47 (2017).
33. J. P. Fadok, M. Markovic, P. Tovote, A. Lüthi, New perspectives on central amygdala function. *Curr. Opin. Neurobiol.* **49**, 141–147 (2018).
34. K. M. McCullough, F. G. Morrison, J. Hartmann, W. A. Carlezon Jr., K. J. Ressler, Quantified coexpression analysis of central amygdala subpopulations. *eNeuro* **5**, ENEURO.0010-18.2018 (2018).
35. T. D. Wilson, S. Valdivia, A. Khan, H.-S. Ahn, A. P. Adke, S. Martinez Gonzalez, Y. K. Sugimura, Y. Carrasquillo, Dual and opposing functions of the central amygdala in the modulation of pain. *Cell Rep.* **29**, 332–346.e5 (2019).
36. W. Haubensak, P. S. Kunwar, H. Cai, S. Ciocchi, N. R. Wall, R. Ponnusamy, J. Biag, H.-W. Dong, K. Deisseroth, E. M. Callaway, M. S. Fanselow, A. Lüthi, D. J. Anderson, Genetic dissection of an amygdala microcircuit that gates conditioned fear. *Nature* **468**, 270–276 (2010).
37. J. Kim, X. Zhang, S. Muralidhar, S. A. LeBlanc, S. Tonegawa, Basolateral to central amygdala neural circuits for appetitive behaviors. *Neuron* **93**, 1464–1479.e5 (2017).
38. H. Li, M. A. Penzo, H. Taniguchi, C. D. Kopec, Z. J. Huang, B. Li, Experience-dependent modification of a central amygdala fear circuit. *Nat. Neurosci.* **16**, 332–339 (2013).
39. M. Venniro, T. I. Russell, L. A. Ramsey, C. T. Richie, H. M. B. Lesscher, S. M. Giovanetti, R. O. Messing, Y. Shaham, Abstinence-dependent dissociable central amygdala microcircuits control drug craving. *Proc. Natl. Acad. Sci. U.S.A.* **117**, 8126–8134 (2020).
40. P. M. Newton, R. O. Messing, Intracellular signaling pathways that regulate behavioral responses to ethanol. *Pharmacol. Ther.* **109**, 227–237 (2006).

41. D. S. Choi, W. Wei, J. K. Deitchman, V. N. Kharazia, H. M. B. Lesscher, T. McMahon, D. Wang, Z. H. Qi, W. Sieghart, C. Zhang, K. M. Shokat, I. Mody, R. O. Messing, Protein kinase Cδ regulates ethanol intoxication and enhancement of GABA-stimulated tonic current. *J. Neurosci.* **28**, 11890–11899 (2008).
42. E. J. Nelson, K. Hellevuo, M. Yoshimura, B. Tabakoff, Ethanol-induced phosphorylation and potentiation of the activity of type 7 adenylyl cyclase: Involvement of protein kinase C δ. *J. Biol. Chem.* **278**, 4552–4560 (2003).
43. V. Pascoli, A. Hiver, R. Van Zessen, M. Loureiro, R. Achargui, M. Harada, J. Flakowski, C. Lüscher, Stochastic synaptic plasticity underlying compulsion in a model of addiction. *Nature* **564**, 366–371 (2018).
44. T. Insel, B. Cuthbert, M. Garvey, R. Heinssen, D. S. Pine, K. Quinn, C. Sanislow, P. Wang, Research domain criteria (RDoC): Toward a new classification framework for research on mental disorders. *Am. J. Psychiatry* **167**, 748–751 (2010).
45. L. E. Kwako, M. L. Schwandt, V. A. Ramchandani, N. Diazgranados, G. F. Koob, N. D. Volkow, C. Blanco, D. Goldman, Neurofunctional domains derived from deep behavioral phenotyping in alcohol use disorder. *Am. J. Psychiatry* **176**, 744–753 (2019).
46. S. H. Ahmed, M. Lenoir, K. Guillem, Neurobiology of addiction versus drug use driven by lack of choice. *Curr. Opin. Neurobiol.* **23**, 581–587 (2013).
47. C. Giuliano, D. Belin, B. J. Everitt, Compulsive alcohol seeking results from a failure to disengage dorsolateral striatal control over behavior. *J. Neurosci.* **39**, 1744–1754 (2019).
48. D. E. Moorman, The role of the orbitofrontal cortex in alcohol use, abuse, and dependence. *Prog. Neuropsychopharmacol. Biol. Psychiatry* **87**, 85–107 (2018).
49. B. J. Everitt, D. M. Hutcheson, K. D. Ersche, Y. Pelloux, J. W. Dalley, T. W. Robbins, The orbital prefrontal cortex and drug addiction in laboratory animals and humans. *Ann. N. Y. Acad. Sci.* **1121**, 576–597 (2007).
50. N. Morisot, K. Phamluong, Y. Ehinger, A. L. Berger, J. J. Moffat, D. Ron, mTORC1 in the orbitofrontal cortex promotes habitual alcohol seeking. *eLife* **8**, e51333 (2019).
51. G. de Guglielmo, E. Crawford, S. Kim, L. F. Vendruscolo, B. T. Hope, M. Brennan, M. Cole, G. F. Koob, O. George, Recruitment of a neuronal ensemble in the central nucleus of the amygdala is required for alcohol dependence. *J. Neurosci.* **36**, 9446–9453 (2016).
52. C. Möller, L. Wiklund, W. Sommer, A. Thorsell, M. Heilig, Decreased experimental anxiety and voluntary ethanol consumption in rats following central but not basolateral amygdala lesions. *Brain Res.* **760**, 94–101 (1997).
53. L. R. Halladay, A. Kocharian, P. T. Piantadosi, M. E. Authement, A. G. Lieberman, N. A. Spitz, K. Coden, L. R. Glover, V. D. Costa, V. A. Alvarez, A. Holmes, Prefrontal regulation of punished ethanol self-administration. *Biol. Psychiatry* **87**, 967–978 (2020).
54. D. C. Blanchard, R. J. Blanchard, Ethoexperimental approaches to the biology of emotion. *Annu. Rev. Psychol.* **39**, 43–68 (1988).
55. E. P. Zorrilla, G. F. Koob, Impulsivity derived from the dark side: Neurocircuits that contribute to negative urgency. *Front. Behav. Neurosci.* **13**, 136 (2019).
56. K. Yu, S. Ahrens, X. Zhang, H. Schiff, C. Ramakrishnan, L. Fenno, K. Deisseroth, F. Zhao, M.-H. Luo, L. Gong, M. He, P. Zhou, L. Paninski, B. Li, The central amygdala controls learning in the lateral amygdala. *Nat. Neurosci.* **20**, 1680–1685 (2017).
57. J.-N. Li, P. L. Sheets, The central amygdala to periaqueductal gray pathway comprises intrinsically distinct neurons differentially affected in a model of inflammatory pain. *J. Physiol.* **596**, 6289–6305 (2018).
58. M. A. Penzo, V. Robert, B. Li, Fear conditioning potentiates synaptic transmission onto long-range projection neurons in the lateral subdivision of central amygdala. *J. Neurosci.* **34**, 2432–2437 (2014).
59. B. Li, Central amygdala cells for learning and expressing aversive emotional memories. *Curr. Opin. Behav. Sci.* **26**, 40–45 (2019).
60. M. J. Hawrylycz, E. S. Lein, A. L. Guillozet-Bongaarts, E. H. Shen, L. Ng, J. A. Miller, L. N. van de Lagemaat, K. A. Smith, A. Ebbert, Z. L. Riley, C. Abajian, C. F. Beckmann, A. Bernard, D. Bertagnolli, A. F. Boe, P. M. Cartagena, M. M. Chakravarty, M. Chapin, J. Chong, R. A. Dalley, B. D. Daly, C. Dang, S. Datta, N. Dee, T. A. Dolbeare, V. Faber, D. Feng, D. R. Fowler, J. Goldy, B. W. Gregor, Z. Haradon, D. R. Haynor, J. G. Hohmann, S. Horvath, R. E. Howard, A. Jeromin, J. M. Jochim, M. Kinnunen, C. Lau, E. T. Lazarz, C. Lee, T. A. Lemon, L. Li, Y. Li, J. A. Morris, C. C. Overly, P. D. Parker, S. E. Parry, M. Reding, J. J. Royall, J. Schulkin, P. A. Sequeira, C. R. Slaughterbeck, S. C. Smith, A. J. Sodt, S. M. Sunkin, B. E. Swanson, M. P. Vawter, D. Williams, P. Wohnoutka, H. R. Zielke, D. H. Geschwind, P. R. Hof, S. M. Smith, C. Koch, S. G. N. Grant, A. R. Jones, An anatomically comprehensive atlas of the adult human brain transcriptome. *Nature* **489**, 391–399 (2012).
61. E. Augier, R. S. Dulman, E. Singley, M. Heilig, A method for evaluating the reinforcing properties of ethanol in rats without water deprivation, saccharin fading or extended access training. *J. Vis. Exp.* 53305 (2017).
62. J. Wolffgramm, A. Heyne, From controlled drug intake to loss of control: The irreversible development of drug addiction in the rat. *Behav. Brain Res.* **70**, 77–94 (1995).
63. C. P. Richter, K. H. Campbell, Alcohol taste thresholds and concentrations of solution preferred by rats. *Science* **91**, 507–508 (1940).
64. P. V. Piazza, J. M. Deminiere, M. Le Moal, H. Simon, Factors that predict individual vulnerability to amphetamine self-administration. *Science* **245**, 1511–1513 (1989).
65. D. Belin, A. C. Mar, J. W. Dalley, T. W. Robbins, B. J. Everitt, High impulsivity predicts the switch to compulsive cocaine-taking. *Science* **320**, 1352–1355 (2008).
66. G. Paxinos, C. Watson, *The Rat Brain in Stereotaxic Coordinates: The New Coronal Set* (Elsevier Academic Press, 2005).
67. X. Li, T. Zeric, S. Kambhampati, J. M. Bossert, Y. Shaham, The central amygdala nucleus is critical for incubation of methamphetamine craving. *Neuropsychopharmacology* **40**, 1297–1306 (2015).
68. L. Ye, W. E. Allen, K. R. Thompson, Q. Tian, B. Hsueh, C. Ramakrishnan, A.-C. Wang, J. H. Jennings, A. Adhikari, C. H. Halpern, I. B. Witten, A. L. Barth, L. Luo, J. A. McNab, K. Deisseroth, Wiring and molecular features of prefrontal ensembles representing distinct experiences. *Cell* **165**, 1776–1788 (2016).
69. H. Kayyal, A. Yiannakas, S. Kolatt Chandran, M. Khamaisy, V. Sharma, K. Rosenblum, Activity of insula to basolateral amygdala projecting neurons is necessary and sufficient for taste valence representation. *J. Neurosci.* **39**, 9369–9382 (2019).
70. S. Pati, S. S. Salvi, M. Kallianpur, B. Vaidya, A. Banerjee, S. Maiti, J. P. Clement, V. A. Vaidya, Chemogenetic activation of excitatory neurons alters hippocampal neurotransmission in a dose-dependent manner. *eNeuro* **6**, ENEURO.0124–ENEU19.2019 (2019).
71. K. Björk, S. T. Saarikoski, C. Arlinde, L. Kovanen, D. Osei-Hyiaman, M. Ubaldi, M. Reimers, P. Hyytiä, M. Heilig, W. H. Sommer, Glutathione-S-transferase expression in the brain: Possible role in ethanol preference and longevity. *FASEB J.* **20**, 1826–1835 (2006).
72. K. J. Livak, T. D. Schmittgen, Analysis of relative gene expression data using real-time quantitative PCR and the $2^{-\Delta\Delta CT}$ method. *Methods* **25**, 402–408 (2001).
73. J. A. Hartigan, P. M. Hartigan, The dip test of unimodality. *Ann. Stat.* **13**, 70–84 (1985).
74. M. Ester, H. Kriegel, J. Sander, X. Xu, A density-based algorithm for discovering clusters in large spatial databases with noise, in *Proc. of 2nd International Conference on Knowledge Discovery and Data Mining (KDD-96)* (AAAI Press, United States, 1996), pp. 226–231.

Acknowledgments

Funding: This study was supported by Swedish Research Council 2013-07434, 2019-01138; Wallenberg Foundation (M.H.); Lions Research Funding (E.D.); Intramural Research Program, NIDA-NIH (Y.S.); and Swedish Research Council 2018-02320 (E.A.). **Author contributions:** E.D., E.A., and M.H. jointly conceptualized and designed the studies. E.D. and M.H. designed and supervised experiments, and analyzed and interpreted results. E.D., L.X., S.T., and F.G. performed the behavioral experiments and analysis. E.D., L.X., and A.N. performed the molecular analyses. E.D., E.B., and L.X. performed surgeries. L.H., E.D., and L.X. performed the perfusions. M.V., Y.S., and R.O.M. generated the shRNA for *Prkcd* and participated in manuscript preparation. E.V. and M.C.v.d.O. provided the viral cocktail and advice for the TRAP approach. E.D. and M.H. drafted the manuscript. All authors have read and approved the manuscript. **Competing interests:** M.H. has received consulting fees, research support, or other compensation from Indivior, Camurus, BrainsWay, Aelis Farma, and Janssen Pharmaceuticals. The other authors declare that they have no competing interests. **Data and materials availability:** All data needed to evaluate the conclusions in the paper are present in the paper and/or the Supplementary Materials.

Submitted 3 February 2021
Accepted 28 June 2021
Published 18 August 2021
10.1126/sciadv.abg9045

Citation: E. Domi, L. Xu, S. Toivainen, A. Nordeman, F. Gobbo, M. Venniro, Y. Shaham, R. O. Messing, E. Visser, M. C. van den Oever, L. Holm, E. Barbier, E. Augier, M. Heilig, A neural substrate of compulsive alcohol use. *Sci. Adv.* **7**, eabg9045 (2021).